

Electronic stopping in astrophysical fusion reactions

C.A. Bertulani *

*National Superconducting Cyclotron Laboratory,
Michigan State University, East Lansing, MI 48824, USA*

(Dated: January 3, 2004)

Abstract

The stopping power of protons and deuterons in low energy collisions with helium gas targets is investigated with the numerical solution of the time-dependent Schrödinger coupled-channels equations using molecular orbital wavefunctions. It is shown that at low projectile energies the energy loss is mainly due to nuclear stopping, charge exchange, and the excitation of low energy levels in the target. The second and third mechanisms, called electronic stopping, dominate for $E_{lab} \geq 200$ eV. At lower energies it is also shown that a threshold effect is responsible for a quick drop of the energy loss. This investigation sheds more light on the long standing electron screening problem in fusion reactions of astrophysical interest.

PACS numbers: 26.20.+f,34.50.Bw

Keywords:

* e-mail: bertulani@nscl.msu.edu

Nuclear fusion reactions proceed in stars at extremely low energies, e.g. of the order of 10 keV in our sun [1, 2]. At such low energies it is extremely difficult to measure the cross sections for charged particles at laboratory conditions due to the large Coulomb barrier. Moreover, laboratory measurements of low energy fusion reactions are strongly influenced by the presence of the atomic electrons. One has observed experimentally a large discrepancy between the experimental data and the best models available to treat the screening effect by the electrons in the target nuclei [3]. The screening effect arises because as the projectile nucleus penetrates the electronic cloud of the target the electrons become more bound and the projectile energy increases by energy conservation. Since fusion cross sections increase strongly with the projectile's energy, this tiny amount of energy gain (of order of 10-100 eV) leads to a large effect on the measured cross sections. However, in order to explain the experimental data it is necessary an extra-amount of energy about twice the expected theoretical value [3].

In order to extract the fusion cross sections from experiment one needs to correct for the energy loss in the target to assign the correct projectile energy value for the reaction. The authors in refs. [4] and [5] have shown that a possible solution to the long standing discrepancy between theory and experiment for the reaction ${}^3\text{He}(d, p){}^4\text{He}$ could be obtained if the projectile energy loss by electronic excitations and charge exchange with the target atoms would be smaller than previously assumed in the experimental data analysis. There have been indeed a few experiments in which evidences of smaller than expected electronic stopping power were reported (see, e.g. ref. [6]). Other reactions of astrophysical interest (e.g., those listed in by Rolfs and collaborators [7, 8]) should also be corrected for this effect. Whereas at higher energies the stopping is mainly due to the ionization of the target electrons, at the astrophysical energies it is mainly due to excitations of the lowest levels, charge-exchange between the target and the projectile, and the nuclear stopping power.

In this work I address the problem of the stopping of very low energy ions in matter. I consider the systems $p+{}^4\text{He}$ and $d+{}^3\text{He}$, for which there are experimental data available. A previous work [9] studied the energy loss of protons on hydrogen gas targets and showed that the stopping at very low proton energies is indeed smaller than what would be expected from extrapolations based on the Andersen and Ziegler tables [10]. The case of helium targets is more complicated due to the electron-electron interaction.

The present approach is based on the solution of the time-dependent Schrödinger equation

for the electron in a dynamical two-center field. The transition from the separated atoms ($H^+ + He$) and the united atom (Li^+) is obtained in the adiabatic approximation, i.e. by assuming that the electronic motion is fast compared to the nuclear separation motion so that the molecular orbitals (MO) are those for the distance $R(t)$ between the nuclei. The atomic wavefunctions, $\phi_\mu = \sum_j c_{j\mu} \phi_j^{Slat}$, are constructed as a linear combination of Slater-type orbitals (STO) [11] of the form $\phi_n^{Slat} = N r^{n-1} \exp(-\zeta r) Y_{lm}(\hat{\mathbf{r}})$, where the Slater coefficients n and ζ are chosen to best approximate the exact atomic wavefunctions (see, e.g. ref. [11]). The molecular orbital wavefunctions for the $p+He$ system, are obtained with the ϕ_μ 's chosen so that half of the STO's are centered on the proton (A) and the other half are centered on the helium nucleus (B). The total wavefunction for the two-electron system is finally written as a Slater determinant of the molecular orbital wavefunctions,

$$\psi_e(\mathbf{r}_1, \mathbf{r}_2, R) = \frac{1}{\sqrt{2}} \begin{vmatrix} \phi_1^{MO}(1)\alpha(1) & \phi_2^{MO}(1)\beta(1) \\ \phi_1^{MO}(2)\alpha(2) & \phi_2^{MO}(2)\beta(2) \end{vmatrix}, \quad (1)$$

where α, β denote the spin state of the electron. Configuration-interaction with double excitation configurations were included in the calculation, with the coefficients n and the Slater parameters ζ chosen in a variational method to obtain the lowest energy states of the system.

Using these conditions and variation method, one obtains the following Hatree-Fock equation: $\mathbf{F} \otimes \mathbf{C} = \mathbf{O} \otimes \mathbf{C} \otimes \mathbf{E}$, where \mathbf{F} is the ‘‘Fock’’ matrix

$$F_{\mu\nu} = H_{\mu\nu} + \sum_{\lambda\sigma} P_{\lambda\sigma} \left[\left\langle \mu\nu \left| \frac{1}{r_{12}} \right| \lambda\sigma \right\rangle - \frac{1}{2} \left\langle \mu\lambda \left| \frac{1}{r_{12}} \right| \nu\sigma \right\rangle \right], \quad P_{\lambda\sigma} = 2 \sum_{i=1}^{occ} c_{\lambda i} c_{\sigma i}, \quad (2)$$

in which ‘‘occ’’ refers to the occupied molecular orbital,

$$H_{\mu\nu} = \int \int \phi_\mu(1) \left[-\frac{1}{2} \nabla^2 - \sum_{L=A,B} \frac{1}{r_{1L}} \right] \phi_\nu(1) d\tau_1, \quad (3)$$

is the one-electron integral and

$$\left\langle \mu\nu \left| \frac{1}{r_{12}} \right| \lambda\sigma \right\rangle = \int \int \phi_\mu(1) \phi_\nu(1) \frac{1}{r_{12}} \phi_\lambda(2) \phi_\sigma(2) d\tau_1 d\tau_2, \quad (4)$$

are the two-electron integrals. The \mathbf{C} matrix is the coefficient matrix $c_{\mu\nu}$ and \mathbf{O} is the overlap matrix $\langle \phi_\mu(1) | \phi_\nu(1) \rangle$. \mathbf{E} is a diagonal matrix with each diagonal element corresponding to the energy of the associated molecular orbital. Solving the Hartree-Fock equations one

obtains the coefficients c_{ij} which give the proper linear combination of atomic orbitals to form the molecular orbital. The energy of the molecular orbitals are then given by

$$E(R) = \sum_{\mu\nu} P_{\mu\nu} H_{\mu\nu} + \frac{1}{2} \sum_{\mu\nu\lambda\sigma} P_{\mu\nu} P_{\lambda\sigma} \left[\left\langle \mu\nu \left| \frac{1}{r_{12}} \right| \lambda\sigma \right\rangle - \frac{1}{2} \left\langle \mu\lambda \left| \frac{1}{r_{12}} \right| \nu\sigma \right\rangle \right]. \quad (5)$$

Table I shows the states involved in the calculation where it is shown how the states in the separated hydrogen and helium atoms become molecular states in the united atom system. For large distances between the nuclei, $R > 15$ a.u. (1 a.u. of length = 0.53 Å) the energy levels for the 1s, 2s, and 2p states of H and He are reproduced to within 2% and 4% of the spectroscopic data, respectively. The energies of these states are shown in figure 1 as a function of the internuclear distance R .

Separated atom	United atom
$\text{H}^+ + \text{He}(1s^2)$	0Σ
$\text{H}(1s) + \text{He}^+(1s)$	1Σ
$\text{H}^+(1s) + \text{He}(1s2s)$	2Σ
$\text{H}(n=2) + \text{He}^+(1s)$	1Π
$\text{H}(n=2) + \text{He}^+(1s)$	3Σ
$\text{H}(n=2) + \text{He}^+(1s)$	4Σ
$\text{H}^+ + \text{He}(1s1p)$	5Σ
$\text{H}^+ + \text{He}(1s1p)$	2Π

Table 1 - Lowest states in the p+He molecule.

At very low proton energies ($E_p \lesssim 10$ keV) it is fair to assume that only the low-lying states are involved in the electronic dynamics. Only for bombarding energies larger than 25 keV the proton velocity will be comparable to the electron velocity, $v_e \simeq \alpha c$. Thus, the evolution of the system is almost adiabatic at $E_p \lesssim 10$ keV. Also shown in figure 1 (inset) are the intersection points of the states with same symmetry. In a fast collision these states would cross (diabatic collisions), whereas in collisions at very low energies (adiabatic collisions) they obey the von Neumann-Wigner non-crossing rule.

In the dynamical case the full time-dependent wavefunction for the system can be expanded in terms of two-center states, $\psi_n(\mathbf{r}_1, \mathbf{r}_2, t)$, given by eq. 1, with expansion coefficients $a_n(t)$. It is further assumed that the nuclei follow a classical straight-line trajectory determined by an impact parameter b , so that the time dependence of the molecular wavefunctions

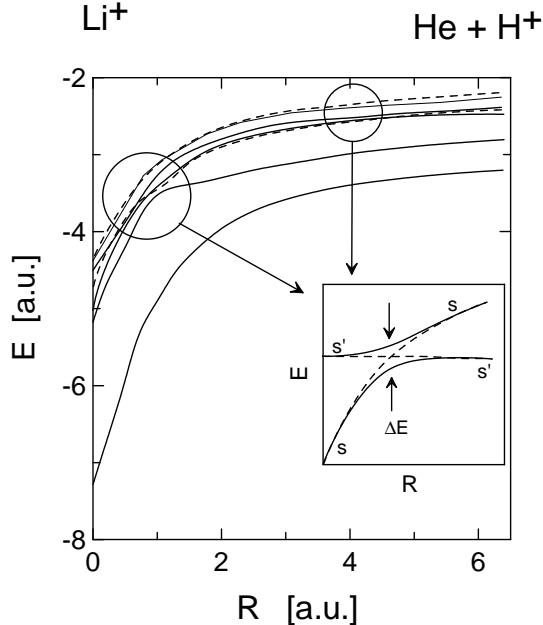


FIG. 1: Adiabatic energies (1 a.u. of energy = 27.2 eV, 1 a.u. of length = 0.53 Å) for the electronic orbitals for the $(\text{H-He})^+$ system as a function of the internuclear separation. As the atoms approach each other slowly curves of same symmetry repel each other. A transition between states s and s' can occur in a slow collision. In a fast collision a diabatic transition, with the states crossing each other, will occur. This is shown in the inset.

is determined by the condition $R = \sqrt{b^2 + v^2 t^2}$, where v is the collision velocity. The dynamical evolution of the H+He system is calculated using the same approach as described in ref. [9]. We solve the set of linear coupled equations

$$i\mathbf{S} \cdot \frac{d\mathbf{A}}{dt} = \mathbf{M} \cdot \mathbf{A} \quad (6)$$

where the column matrix \mathbf{A} represents the time-dependent expansion coefficients, \mathbf{S} is the overlap matrix with elements $S_{ij} = \langle \psi_i | \psi_j \rangle$ and \mathbf{M} is the coupling matrix with elements $M_{ij} = \langle \psi_i | H_{el} - i\partial/\partial t | \psi_j \rangle$, where H_{el} is the electronic Hamiltonian. The solutions are obtained starting from initial internuclear distance of 15 a.u. for the incoming trajectory and stopped at the same value for the outgoing trajectory. The probability for the capture in the proton is obtained by a projection of the final wavefunction into the wavefunctions of

the $1s$, $2s$ and $2p$ states of the hydrogen atom.

$$P_{exch} = \left| \sum_m a_m(\infty) \langle \psi_H | \psi_m(\infty) \rangle \right|^2. \quad (7)$$

Resonant charge-exchange in atomic collisions was first observed by Everhart and collaborators [12]. In these experiments it was determined that the exchange probability in homonuclear atomic collisions oscillates with the incoming energy for a collision with a given impact parameter, or scattering angle. This was interpreted [13] as due to transitions between degenerate states of the system at large internuclear separation distance. In the simplest situation of a $p + H$ the degenerate states are the symmetric and antisymmetric states obtained from the linear combination of the (H^+H) and (HH^+) wavefunctions. This effect was studied in ref. [14], where a relation between the damping of the oscillatory behavior of the exchange probabilities and the Landau-Zener effect was established. The $p + H$ collisions at small energies was recently studied in ref. [9] and the oscillatory effect was shown to be related to the Sommerfeld quantization rule for the integral from $t = -\infty$ to $t = \infty$ of the energy difference between the symmetric and antisymmetric state. The electron tunnels back and forth between the projectile and the target during the ingoing and the outgoing parts of the trajectory. When the interaction time is an exact multiple of the oscillation time, a minimum in the exchange probability occurs.

A similar situation occurs for $p + He$ collisions, as shown in figure 2 for the electron capture probability by the proton at 10 keV bombarding energy. These oscillations are due to the electron exchange between the ground state of the hydrogen and the first excited state in He ($1s2s$). But, in contrast to the H^+H system, the oscillations are strongly damped. Following the work of Lichten [14] we interpret this damping effect as due to the interference between the participant states and a band of states of average energy $\langle E_a \rangle$ and width 2Γ , as seen in figure 1. The important regions where the diabatic level cross occurs is shown in figure 1 inside the encircled areas. The damping mechanism is best understood using the Landau-Zener theory for level crossing. At the crossing there is a particular probability $(1 - P)$ of an adiabatic transition where P is given by the Landau-Zener formula

$$P_{exch} = \exp \left[\frac{2\pi H_{ss'}^2}{v (d/dR) (E_s - E_{s'})} \right] \quad (8)$$

where v is the collision velocity and $H_{ss'}$ is the off-diagonal matrix element connecting states s and s' . The oscillatory behavior shown in figure 2 is due to the many level transitions

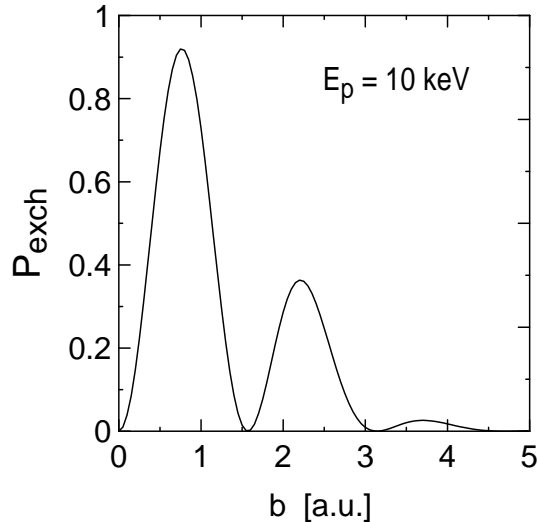


FIG. 2: Probability of charge exchange in the collision $p+{}^4\text{He}$ showing the resonant behavior as a function of the impact parameter and for proton energy $E_p = 10$ KeV.

at the crossing, each time governed by the probability of eq. 8. The interference with the neighboring states introduces a damping in the charge exchange probability, i.e.

$$P_{exch}(b, t) \simeq \cos^2 \left(\frac{\langle E_a \rangle b}{v} \right) \exp \left[-\frac{2\pi\Gamma^2 b}{v \langle E_a \rangle} \right],$$

where $\langle E_a \rangle \simeq 1$. a.u. is the average separation energy between the 0Σ level and the bunch of higher energy levels shown in figure 1. The exponential damping factor agrees with the numerical calculations if one uses $\Gamma \simeq 5$ eV, which agrees with the energy interval of the band of states shown in figure 1.

The total cross section for charge exchange is calculated from

$$\sigma = 2\pi \int P_{exch} b db .$$

The numerical results for the $p + \text{He}$ system is shown in figure 3 as a function of the proton energy. The solid line is the result of using the coupled-channels equations 6, and 7 for the exchange probability. The experimental data are from ref. [15]. We observe that the calculation reproduces the trend of the experimental data. But, whereas the maximum of the cross section at $E_p \simeq 20$ keV is rather well described, the calculations underestimate the cross sections at smaller energies. The low energy slope of the cross section is nonetheless well reproduced. At energies higher than the Bragg peak ($E_p \gtrsim 20$ keV) the numerical results

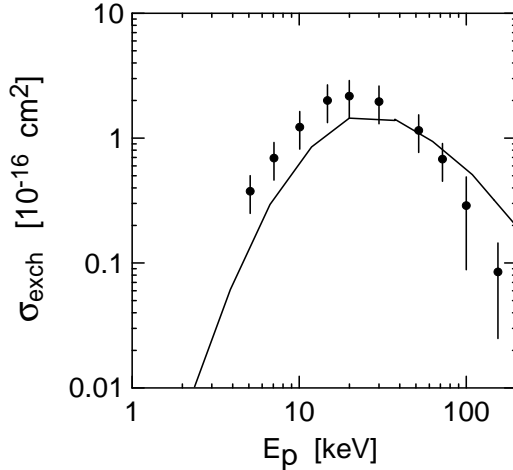


FIG. 3: Charge-exchange cross sections for the $p + {}^4\text{He}$ as a function of the proton energy. The solid line was obtained by solving the coupled-channels equations 6, and using 7 for the exchange probability. The experimental data are from ref. [15].

should not be trusted as the adiabatic approximation for the molecular orbitals and also the inclusion of only the lowest energy levels are not adequate (continuum states should also be included). For $E_p \rightarrow 0$, the charge exchange cross section must go to zero since the higher binding of the electrons in He prevents the capture by the incident proton in an extreme adiabatic collision. This feature is correctly reproduced by the numerical calculations.

In figure 4 we show the stopping cross section of the proton. The experimental data are from refs. [15, 16]. The stopping cross section is defined as $S = \sum_i \Delta E_i \sigma_i$, where ΔE_i is the energy loss of the projectile in a process denoted by i . The stopping power, $S_P = dE/dx$, the energy loss per unit length of the target material, is related to the stopping cross section by $S = S_P/N$, where N is the atomic density of the material. In the charge exchange mechanism one of the electrons in He is transferred to incoming proton and the energy loss by the proton is given by $\Delta E = m_e v^2/2$, where v is the proton velocity. Assuming that there are few free electrons in the material (e.g. in the helium gas) only one more stopping mechanism at very low energies should be considered: the nuclear stopping power, S_n . This is simply the elastic scattering of the projectile off the target nuclei. The projectile energy is partially transferred to the recoil energy of the target atom. The stopping cross section for this mechanism has been extensively discussed in ref. [17]. The total stopping power is

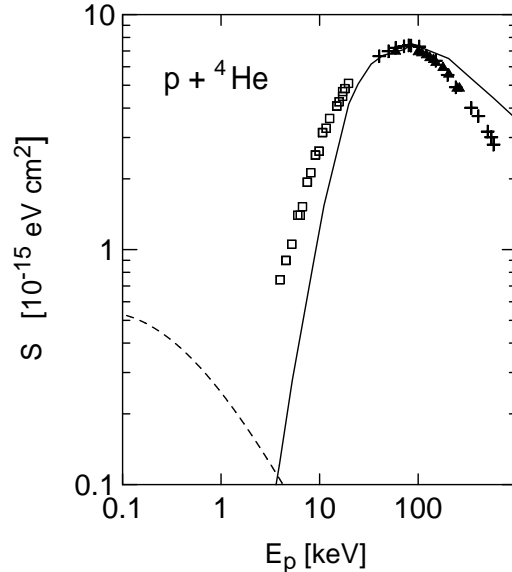


FIG. 4: Stopping cross section for proton incident on gas ${}^4\text{He}$ targets, as a function of the proton energy. The experimental data are from refs. [15, 16].

given by $S = S_{exch} + S_n$. In units of 10^{-5} eV cm^2 the nuclear stopping for the $p+{}^4\text{He}$ system at $E_p < 30$ keV is given by

$$S_n = S_0 \frac{\ln(1 + 1.1383\varepsilon)}{(\varepsilon + 0.01321\varepsilon^{0.21226} + 0.19593\varepsilon^{0.5})}, \quad (9)$$

where $S_0 = 0.779$ and $\varepsilon = 5.99E_p$, with the proton incident energy E_p given in keV.

The dashed line in figure 4 gives the energy transfer by means of nuclear stopping, while the solid line shows the results for the electronic stopping mechanism, i.e. due to charge-exchange and excitation in the helium target. We see that the nuclear stopping dominates at the lowest energies, while the electronic stopping is larger for proton energies greater than 200 eV. We do not consider the change of the charge state of the protons as they penetrate the target material. The exchange mechanism transforms the protons into H atoms. These again interact with the target atoms. They can loose their electron again by transferring it back to a bound state in the target.

At very low energies the only possibility that the electron is captured by the proton is if there is a transition $1s^2({}^1S_0) \rightarrow 1s2s({}^3S)$ in the helium target. Only in this case the energy of one of the electrons in helium roughly matches the electronic energy of the ground state in H. This resonant transfer effect is responsible for the large capture cross sections.

When this transition is not possible the electrons prefer to stay in the helium target, as the energy of the whole system is lowest in this case. Another possible mechanism for the stopping is the excitation of the helium atom by the transition $1s^2(^1S_0) \longrightarrow 1s2s(^3S)$. Thus, there must be a direct relationship between the energy transfer to the transition $1s^2(^1S_0) \longrightarrow 1s2s(^3S)$ and the minimum projectile energy which enables electronic changes. Ref. [18] reported for the first time this effect, named by threshold energy, which can be understood as follows. The momentum transfer in the projectile-target collision, Δq , is related to the energy transfer to the electrons by $\Delta q = \Delta E/v$, where v is the projectile velocity. In order that this momentum transfer absorbed by the electron, induces an atomic transition, it is necessary that $\hbar^2 \Delta q^2 / 2m_e \sim \Delta E$. Solving these equations for the projectile energy one finds

$$E_p^{thres} \sim \frac{m_p}{4m_e} \Delta E . \quad (10)$$

This is the threshold energy for atomic excitations and/or charge exchange. If the projectile energy is smaller than this value, no stopping should occur. The energy for transition $1s^2(^1S_0) \longrightarrow 1s2s(^3S)$ in He is $\Delta E = 18.7$ eV. Thus, for p + He collisions, the threshold energy is $E_p^{thres} \sim 9$ keV. This roughly agrees with the numerical calculations presented in figure 4 (solid curve).

Figure 5 shows the energy loss of deuterons in ^3He gas as a function of deuteron energy. The data are from ref. [18]. The solid curve is the numerical calculation for the electronic stopping power, while the dashed curve shows the nuclear stopping. For this system the coefficients in eq. 9 are $S_0 = 1.557$ and $\varepsilon = 4.491 E_d$, respectively. As discussed in ref [18] the threshold deuteron energy in this reaction is of the order of 18 keV, which agrees with the estimate based on eq. 10. However, the numerical calculations based on the electronic stopping (solid curve of fig. 5) indicate a lower threshold energy for this system. Nonetheless, the agreement with the experimental data is very good for $E_d > 20$ keV. The threshold effect is one more indication that the extrapolation $S \sim v$, based on the Andersen-Ziegler tables is not applicable to very low energies.

The steep rise of the fusion cross sections at astrophysical energies amplifies all effects leading to a slight modification of the projectile energy [19]. The results presented in this article show that the stopping mechanism does not follow a universal pattern for all systems. The threshold effect reported in ref. [18] is indeed responsible for a rapid decrease of the electronic stopping at low energies. It will occur whenever the charge-exchange mechanism

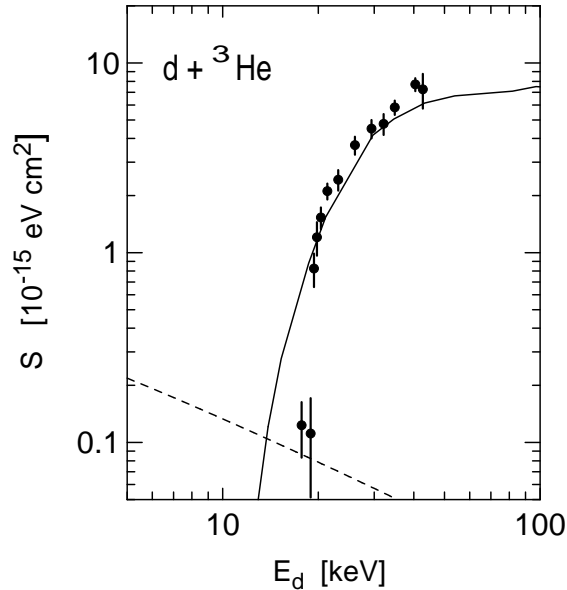


FIG. 5: Energy loss of deuterons in ^3He gas as a function of deuteron energy. Data are from ref. [18]. The solid curve is the calculation for the electronic stopping power, while the dashed curve shows the nuclear stopping.

and the excitation of the first electronic state in the target involve approximately the same energy. However, the drop of the electronic stopping is not as sharp as expected from the simple classical arguments given by eq. 10.

The experiments on astrophysical fusion reactions have shown that the screening effect is much larger than expected by theory. The solution to this problem might be indeed the smaller stopping power, due to a steeper slope at low energies induced, e.g. by the threshold mechanism. This calls for improved theoretical studies of the energy loss of ions at extremely low energies of and for their independent experimental verification. The present situation is highly disturbing because if we cannot explain the laboratory screening effect, most likely we cannot explain it in stellar environments.

I would like to express my gratitude to D.T. de Paula and I. Ivanov for helping me with the programming during the earlier stages of this work. This work was supported by the

- [1] D.D. Clayton, *Principles of Stellar Evolution and Nucleosynthesis*, McGraw-Hill, New York, 1968.
- [2] C. Rolfs and W.S. Rodney, *Cauldrons in the Cosmos*, Chicago Press, Chicago, 1988.
- [3] C. Rolfs, Prog. Part. Nucl. Phys. **46**, 23 (2001).
- [4] K. Langanke, T.D. Shoppa, C.A. Barnes and C. Rolfs, Phys. Lett. **B369**, 211 (1996).
- [5] J.M. Bang, L.S. Ferreira, E. Maglione, and J.M. Hansteen, Phys. Rev. **C53**, R18 (1996).
- [6] R. Golser and D. Semrad, Phys. Rev. Lett. **14**, 1831 (1991).
- [7] H.J. Assenbaum, K. Langanke, and C. Rolfs, Z. Phys. **A327**, 461 (1987).
- [8] E. Somorjai and C. Rolfs, Nucl. Instrum. Meth. **B99**, 297 (1995).
- [9] C.A. Bertulani and D.T. de Paula, Phys. Rev. **C 62**, 045802 (2000).
- [10] H.H. Andersen and J.F. Ziegler, "Hydrogen stopping powers and ranges of ions in matter, Vol. 3, Pergamon press, New York (1977).
- [11] I.N. Levine, *Quantum Chemistry*, 5th ed., Prentice Hall (2000).
- [12] G.J. Lockwood, G.H. Morgan, and E. Everhart, Phys. Rev. **118** (1950) 1552; F.P. Ziemba and E. Everhart, Phys. Rev. Lett. **2** (1999) 299; G.J. Lockwood and E. Everhart, Phys. Rev. **125** (1962) 567.
- [13] T. Holstein, J. Phys. Chem. **56** (1952) 832.
- [14] W. Lichten, Phys. Rev. **131** (1963) 229.
- [15] M.E. Rudd et al., Phys. Rev. **A 28**, 3244 (1983).
- [16] J.T. Park and E.J. Zimmerman, Phys. Rev. **131**, 1611 (1963).
- [17] J.F. Ziegler, J.P. Biersack and U. Littmark, "The stopping and range of ions in matter", Vol. 1, Pergamon Press, New York (1985).
- [18] A. Formicola et al., Eur. Phys. J. **A8**, 443 (2000).
- [19] A. B. Balantekin, C. A. Bertulani, M. S. Hussein, Nucl. Phys. **A627**, 324 (1997).